time resolution and can no longer consider that the resonance decays after the direct background scattering.

The first use of this with which I am familiar—and it was illuminating to me as I was working on the same problem and missed the point completely—was in the work of Feshbach, Porter, and Weisskopf, who showed that narrow elastic-scattering resonances could be considered as inelastic, absorptive factors if one averaged over broad energy intervals. You are then using good time resolution and the scattering by the long lived, narrow, resonances is incoherent with the incident beam, just as inelastic processes.

PHILLIPS: The point I tried to make this morning is that interference effects occur if you are not absolutely sure that a particle is first-emitted, or whether it is second-emitted—and I think that is the probability in this reaction—and also this effect if you don't know the angles of the detectors. I don't know how you can talk about these resonant states, if you don't say that one of them is first-emitted.

ADAIR: The experiments I presented are not troubled by overlapping bands in the Dalitz plot which can lead to interferences which distort widths. When one studies interference effects in a small region of energy on the Dalitz plot, time information is lost and the concept of time order has no meaning. Perhaps we are saying the same thing in complementary ways. It is customary, in high-energy physics, to discuss these reactions in terms of energy, which is the measured quantity, and not in the complementry, but superfluous, and often misleading, terms of time ordering.

DONOVAN: I think it is a misinterpretation of what you mean by good energy resolution, and what Professor Phillips means by good energy resolution. In absolute units it is very different in low-energy and high-energy physics. The important point is whether the energy resolution is comparable with the width of what you are looking at; not whether it is good or bad. And if you are looking at very narrow states, like gamma emitting states, and examining the particle resolution, then it is never good.

REVIEWS OF MODERN PHYSICS VOLUME 37, NUMBER 3 JULY 1965

Peripheral Production and Decay Correlations of Resonances*

J. D. JACKSON
Department of Physics, University of Illinois, Urbana, Illinois

1. QUASI-TWO-BODY CHANNELS IN MULTIPARTICLE FINAL STATES

In reactions produced by the bombardment of nucleons with pions, K mesons, nucleons, and antinucleons, final states involving three or more particles become increasingly important as the bombarding energy is raised. For example, in K^+p collisions at an incident laboratory momentum of 1.96 GeV/c, the total cross section of 19.5 mb is divided among the various final states as follows[1]:

$$K^+p\longrightarrow\begin{cases} K^+p & 7.6\ \text{mb} \\ K^0\pi^+p & 4.6 \\ K^+\pi^0p & 2.0 \\ K^+\pi^+n & 1.6 \\ K^+\pi^+\pi^-p & 1.7 \\ K^0\pi^0\pi^+p & 1.3 \\ K^0\pi^+\pi^+n & 0.33 \\ K^+p(3\pi) & 0.1 \end{cases}.$$

Another example involves 2.9-GeV/c π^+ incident on hydrogen,[2] where some of the final states are

$$\pi^+p\longrightarrow\begin{cases} \pi^+p\pi^0 & 3.6\ \text{mb} \\ \pi^+n\pi^+ & 2.1 \\ \pi^+p\pi^+\pi^- & 3.1 \\ \pi^+p\pi^+\pi^-\pi^0 & 4.1 \\ \pi^+n\pi^+\pi^+\pi^- & 0.56 \end{cases}.$$

One sees from these examples that 3, 4, and even 5 particles in the final state is a common occurrence.[3]

A prominent feature of these reactions is the presence of mesonic and baryonic resonances. Such resonances (the nine vector mesons, ρ, ω, K^*, $\bar{K}^*$, ϕ; the decuplet of isobars, N^*, Y_1^*, Ξ^*, Ω^-; and others) are, with few exceptions, dynamically unstable and are observed only through kinematic correlations of their decay products. A typical example is shown in Fig. 1. The Dalitz plot for the reaction

$$K^+p\longrightarrow K^0\pi^+p,$$

* Supported in part by the U. S. Office of Naval Research under contract ONR 1834(05).

[1] S. Goldhaber, in *Proceedings Athens Topical Conference on Recently Discovered Resonant Particles* (26–27 April 1963), edited by B. A. Munir and L. J. Gallaher (Ohio University Press, Athens, Ohio, 1963), p. 92.

[2] C. Alff, D. Berley, D. Colley, N. Gelfand, U. Nauenberg *et al.*, Phys. Rev. Letters **9**, 322 (1962).

[3] The rather peculiar fact that one of the five particle states ($\pi^+p\pi^+\pi^-\pi^0$) in the π^+p reactions has a greater probability than any of the three- or four-particle states, and almost an order of magnitude greater frequency than another five-particle state has its explanation in the presence of the quasi-two-body process, $\pi^+p\rightarrow\omega N^*$.

produced by 3-GeV/c K^+ mesons incident on a hydrogen bubble chamber[4] indicates the frequent formation of two resonances, the K^* at a mass of 892 MeV in the $K^0\pi^+$ invariant-mass spectrum and the well-known N^* [(3, 3) resonance] at 1238 MeV in the π^+p mass spectrum.[5] Detailed analysis shows that this reaction with three particles in the final state is in fact mainly two quasi-two-body reactions,

$$K^+p\rightarrow K^{*+}p$$

and

$$K^+p\rightarrow K^0N^{*++},$$

which occur with roughly equal probability (~40% each). Only a small fraction of the events are nonresonant. Similar results are obtained at lower energies.[1]

Many other three-particle final states show similar effects. The discovery of the ρ meson[6] in the process, $\pi^-p\rightarrow\pi^-\pi^0p$, is one instance. Others are the presence of ρ^+ and N^{*++} in the reaction, $\pi^+p\rightarrow\pi^0\pi^+p$;[7] the quasi-two-body annihilation of antiprotons stopping in hydrogen via the reaction, $\bar{p}p\rightarrow\rho\pi$,[8] and the formation of K^* in the process, $\pi^-p\rightarrow K^+\pi^-\Sigma^0$.[9] This listing is indicative, not exhaustive.

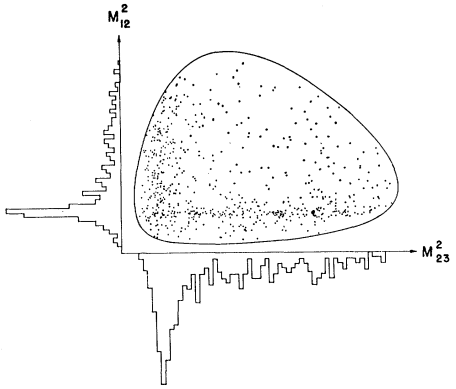

FIG. 1. Dalitz plot and invariant-mass projections for the reaction $K^+p\rightarrow K^0\pi^+p$ at 3 GeV/c, a slightly schematic (but realistic) representation of the data of Ref. 4. The projections show the dominance of K^* formation in the $K^0\pi^+$ system (M_{12}^2 axis) and of N^* in the π^+p system (M_{23}^2 axis).

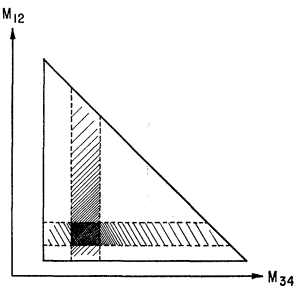

FIG. 2. Kinematical diagram for four-particle final states. With the invariant masses M_{12} and M_{34} of two pairs of particles as variables the allowed region is a triangle. The shading represents schematically the simultaneous production of two resonances (the heavily shaded overlap region), as well as some creation of single resonances independently of the mass of the other pair.

With four particles in the final state, the particles can be grouped in pairs to give a two-dimensional kinematic diagram, in addition to the various one-dimensional invariant mass plots. Figure 2 shows such a diagram. With the invariant masses of the two pairs as variables, the kinematically allowed region is a triangle. Each event corresponds to a single point in the triangle, in a manner analogous to the Dalitz plot for three particles. But there are at least two complications not present in the Dalitz plot: the choice of pairing is arbitrary and the phase-space density is not uniform. Nevertheless the plot has value. Prior experience dictates likely pairings and dramatic effects will still show up. The shading in Fig. 2 represents schematically a common situation in which there is some evidence for a resonance in each of the pairings, independently of the mass of the other pair, but a strong enhancement in the overlap region corresponding to simultaneous creation of both resonances. The CERN K^+p experiment at 3 GeV/c,[4] with approximately 1000 measured $K^+\pi^-\pi^+p$ events, provides a striking illustration. When the pairings ($K^+\pi^-$) and (π^+p) are made, somewhat over 500 events lie in the small region of overlap of the K^* and N^* bands. This means that the quasi-two-body channel,

$$K^+p\rightarrow K^*N^*,$$

accounts for over half the four-prong events. The remainder seem divided more or less equally among $K^*\pi^+p$ (no N^*), $N^*K^+\pi^-$ (no K^*), and nonresonant events. Corresponding effects are seen in π^+p collisions where the simultaneous creation of ρ^0 and N^{*++} occurs appreciably in the reaction $\pi^+p\rightarrow\pi^+\pi^-\pi^+p$ at 2–3 GeV/c,[2] 4 GeV/c,[10] and 8 GeV/c.[11]

The above examples are enough to indicate that quasi-two-body channels, in which one or both of the "particles" in the final state are resonances, are a prominent feature of collisions in the energy range from 1 to 8 GeV. Other, less simple, channels do, of course, exist with sizable intensities. But in this paper we shall

[4] M. Ferro-Luzzi, R. George, Y. Goldschmidt-Clermont, V. P. Henri, B. Jongejans *et al.*, *Proceedings 1963 Sienna International Conference on Elementary Particles* (Italian Physical Society, Bologna, 1963), Vol. I, p. 189; G. R. Lynch, M. Ferro-Luzzi, R. George, Y. Goldschmidt-Clermont, V. P. Henri *et al.*, Phys. Letters **9**, 359 (1964); and papers to be published in Physical Review and Nuovo Cimento.

[5] The invariant-mass plot for the other combination (K^0p) is not shown in Fig. 1. Constant K^0p mass corresponds to a diagonal line on the Dalitz plot since $M_{12}^2+M_{23}^2+M_{31}^2=$constant. The data show no evidence of a K^0p resonance.

[6] A. R. Erwin, R. March, W. D. Walker, and E. West, Phys. Rev. Letters **6**, 628 (1961); Saclay–Orsay–Bari–Bologna collaboration, Nuovo Cimento **25**, 365 (1962).

[7] Aachen – Berlin – Birmingham – Bonn – Hamburg – London – München collaboration, Phys. Letters **10**, 229 (1964); Nuovo Cimento **34**, 495 (1964); Saclay–Orsay–Bari–Bologna collaboration, *Proceedings 1963 Sienna International Conference on Elementary Particles* (Italian Physical Society, Bologna, 1963), Vol. I, p. 239, and preprint (June 1964). See also Refs. 2 and 33.

[8] G. B. Chadwick, W. T. Davies, M. Derrick, C. J. B. Hawkins, J. H. Mulvey *et al.*, in *Proceedings 1962 International Conference on High Energy Physics* (CERN, Geneva, 1962), p. 69.

[9] G. A. Smith, J. Schwartz, D. H. Miller, G. R. Kalbfleisch, R. W. Huff *et al.* Phys. Rev. Letters **10**, 138 (1963).

[10] Aachen–Berlin–Birmingham–Bonn–Hamburg–London–München collaboration, Nuovo Cimento **35**, 659 (1965).

[11] Aachen–Berlin–CERN collaboration, Phys. Letters **12**, 356 (1964).

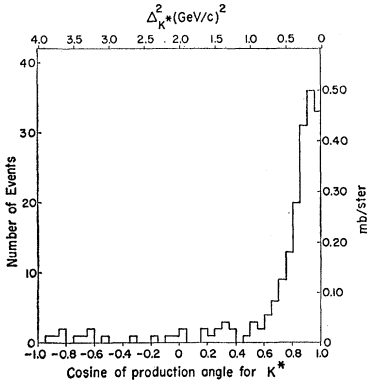

FIG. 3. Differential cross section for production of K^* in the reaction $K^+p\rightarrow K^*p$ at 3 GeV/c. The data are from Ref. 4. The upper (lower) abscissa scale gives the square of the invariant momentum transfer (cosine of the center-of-mass production angle).

focus our attention on quasi-two-body processes involving production of resonances.

2. PERIPHERAL NATURE OF THE PRODUCTION PROCESS AND THE ONE-MESON-EXCHANGE MODEL

Once the existence of a quasi-two-body reaction has been established from the mass plots, the events in the resonant band(s) can be studied for dynamical information. One important aspect is the angular distribution of production. For reactions well above threshold, this distribution is generally peaked very much forward (or backward), corresponding to small momentum transfers. For the reactions whose Dalitz plot are given in Fig. 1 the differential cross sections in the center of mass are shown in Figs. 3 and 4. The angular distributions are confined almost entirely to momentum transfers (Δ^2) less than 0.5 (GeV/c)^2, with an average value of 0.2–0.3 (GeV/c)^2. For the ρ-production reaction, $\pi p\rightarrow\rho N$, the important range of momentum transfers is even smaller, with an average value of 0.10–0.15 (GeV/c)^2, as can be seen from the data in Fig. 6. These examples are typical of the momentum transfer distributions observed for almost all quasi-two-body production reactions at energies of a few GeV.

The predominance of small momentum transfers implies that glancing collisions are most important in these reactions. This fact can be stated in various equivalent ways, depending on the language used: collisions with large impact parameters give rise preferentially to quasi-two-body reactions; such collisions are dominated by high partial waves; the reaction is mediated by a long-range force corresponding to the exchange of a light particle; the production amplitude is dominated by the nearby singularities in the t channel. The latter two modes of description find a natural pictorial representation in the diagram of Fig. 5(a), where the peripheral nature of the process is assumed to result from the predominance of low-mass states e in the t channel (e.g., π exchange, ρ exchange, etc.).

Historically, attention was focused on the one-meson-exchange diagram by the observation of Goebel[12] and Chew and Low[13] that scattering of unstable particles such as pions by pions could be studied provided the one-particle-exchange contribution [Fig. 5(b)] could be isolated by an extrapolation of the production data from the physical region of Δ^2 to the unphysical position, $\Delta^2=-m_{ex}^2$. Experience has shown that the extrapolation procedure is very difficult to apply without further assumptions. The very peripheral nature of the processes implies, however, that the one-particle-exchange diagram may be the main contribution in the physical region, at least for small Δ^2. This is the basis of the one-pion-exchange (OPE) model of Drell,[14] Salzman and Salzman,[15] and Ferrari and Selleri.[16]

The essential feature of the OPE model is the presence in the differential cross section of the square of the pion propagator, $(\Delta^2+m_\pi^2)^{-1}$. The idea that such a factor is responsible for the peaking at small Δ^2 is very attractive, but is not borne out quantitatively by specific calculations. If, for example, the OPE cross section for the reaction, $\pi p\rightarrow\rho p$, is calculated, it is found to have the form,

$$\frac{d\sigma}{d\Delta^2}=\frac{\pi}{4m_\rho^2m_N^2P_{\rm inc}^2}\cdot\frac{g^2}{4\pi}\cdot\frac{G^2}{4\pi}\cdot\frac{\Delta^2[(m_\rho-m_\pi)^2+\Delta^2][(m_\rho+m_\pi)^2+\Delta^2]}{(\Delta^2+m_\pi^2)^2},\quad(1)$$

where m_π, m_ρ, m_N are the masses of the pion, the ρ meson and the nucleon, respectively, $P_{\rm inc}$ is the in-

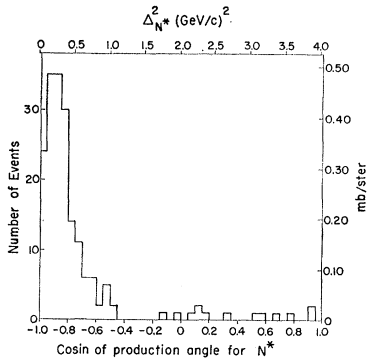

FIG. 4. Same as Fig. 3, but for N^* produced in the reaction $K^+p\rightarrow K^0N^*$ at 3 GeV/c.

[12] C. J. Goebel, Phys. Rev. Letters **1,** 337 (1958).
[13] G. F. Chew and F. E. Low, Phys. Rev. **113,** 1640 (1959).
[14] S. D. Drell, Phys. Rev. Letters **5,** 342 (1960); Rev. Mod. Phys. **33,** 458 (1961).
[15] F. Salzman and G. Salzman, Phys. Rev. **120,** 599 (1960).
[16] E. Ferrari and F. Selleri, Nuovo Cimento Suppl. **24,** 453 (1962); Appendix IV contains many references.

cident pion's momentum in the laboratory, while $g^2/4\pi \simeq 2.0$ is the coupling strength for ρ decay corresponding to $\Gamma_\rho \simeq 100$ MeV and $G^2/4\pi \simeq 14.5$ is the pion–nucleon coupling strength. Since the coupling constants are known the absolute scale and shape are determined. A comparison of Eq. (1) with experiment[17] is shown in Fig. 6. There is gross disagreement with the data, the cross section (1) being too large by nearly a factor of 2 at small Δ^2 and failing to decrease rapidly with increasing Δ^2 (and in fact increasing for $\Delta^2 > 20\mu^2$). This behavior of (1) can be traced to the dependence on Δ^2 in the numerator, the factor Δ^2 coming from the spin-flip inherent in the pion–nucleon coupling and the other factors from the integer spin of the ρ meson. Similar disagreements between the unadorned OPE model and experiment occur for processes like $NN \to NN^*$, $KN \to K^*N^*$. In fact, the larger the spins in the final state, the more powers of Δ^2 in the numerator, and the greater the disagreement.

In their detailed calculations, first for $NN \to NN^*$ and later for $\pi N \to \rho N$, Ferrari and Selleri[16] introduced form factors into the OPE cross section. The argument was that two vertices and the propagator in the OPE diagram [Fig. 5(a)] actually had renormalization effects that involved unknown functions of Δ^2. Hence the perturbation-theory formula was multiplied by a factor $|F(\Delta^2)|^2$, where $F(\Delta^2)$ was an empirical form factor, normalized to unity at the pion pole, $\Delta^2 = -m_\pi^2$, since the coupling constants are defined in terms of a pion on the mass shell. Evidently a suitably chosen function with this normalization can provide the necessary damping for large Δ^2 and reduction in cross section at small Δ^2. By fitting ρ-meson production data at 1.6 GeV/c,[18] Amaldi and Selleri[19] determined an appropriate

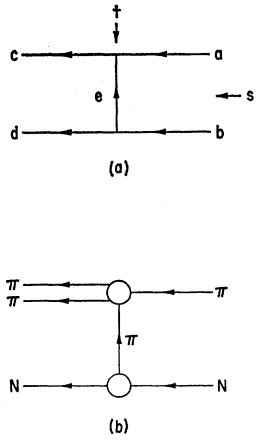

FIG. 5. (a) Feynman diagram for the reaction, $ab \to cd$, in the s channel. The t-channel reaction, $a\bar{c} \to \bar{b}d$, is thought of as proceeding via an intermediate state e which, in the peripheral model, is usually one or two light mesons. (b) One-pion-exchange contribution to the production process, $\pi N \to \pi\pi N$, with pion–pion scattering at the upper vertex.

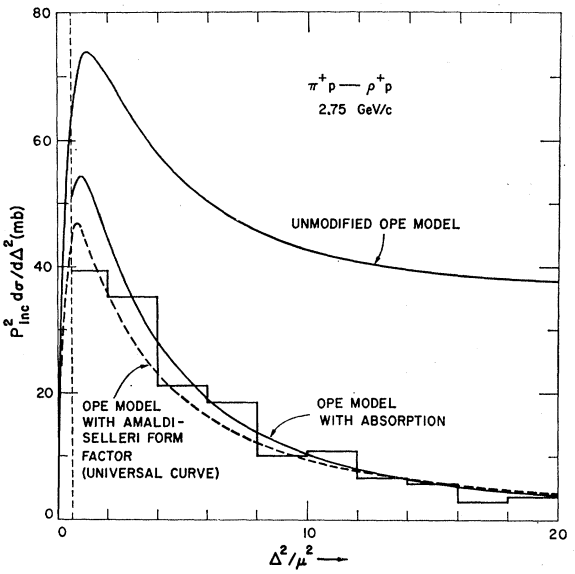

FIG. 6. Comparison of theory and experiment for the differential cross section of the reaction, $\pi^+ p \to \rho^+ p$ at 2.75 GeV/c. The histogram represents the data of Ref. 17. The upper solid curve is the cross section predicted by the unmodified OPE model, Eq. (1). The dashed curve is given by Eq. (1), multiplied by the square of the form factor (2). The lower solid curve is that predicted by the OPE model modified to include absorptive effects as described in Secs. 5 and 6. The abscissa is Δ^2 in units of $\mu^2 = m_\pi^2 = 0.0195$ (GeV/c)^2.

form factor:

$$F(\Delta^2) = \frac{0.72}{1+(\Delta^2+\mu^2)/4.73\mu^2} + \frac{0.28}{1+[(\Delta^2+\mu)/32\mu^2]^2}. \tag{2}$$

Within the framework of the OPE model of Ferrari and Selleri, the differential cross section (1), multiplied by the square of (2), is anticipated to give a reasonable description of the ρ-production data at all incident energies. The dashed curve in Fig. 6 is thus a universal form. We see that it gives an adequate representation of the data at 2.75 GeV/c. Indeed, the agreement with ρ-production data at all energies can be considered adequate, and represents a success for the OPE model with a form factor.

Within the past year or two there has been an accumulation of data on a variety of reactions. One new feature is in evidence. There are reactions which cannot proceed via pion exchange (for example, $\pi^+ p \to \pi^0 N^{*++}$ and $K^+ p \to K^0 N^{*++}$ of Figs. 1 and 4, which presumably go via ρ exchange or a more complicated mechanism). These processes are found to be almost as peripheral in their Δ^2 dependence as those that can utilize pion exchange, whereas cross sections calculated assuming vector meson exchange[20,21] have much broader distribu-

[17] Saclay–Orsay–Bari–Bologna collaboration, in *Proceedings of the XIIth International Conference on High Energy Physics (Dubna, 1964)* (Atomizdat, Moscow, 1965), Abstract VII-42; and private communication.

[18] Saclay–Orsay–Bari–Bologna collaboration, Nuovo Cimento **29**, 515 (1963).

[19] U. Amaldi and F. Selleri, Nuovo Cimento **31**, 360 (1964).

[20] L. Stodolsky and J. J. Sakurai, Phys. Rev. Letters **11**, 90 (1963); L. Stodolsky, Phys. Rev. **134**, B1099 (1964).

[21] J. D. Jackson and H. Pilkuhn, NuovoC imento **33**, 906, (1964); **34**, 1841E (1964).

tions, characteristic of the greater mass of the exchanged particle (see, for example, Fig. 6 of Ref. 21). Again empirical form factors can be employed to bring theory and experiment into agreement. But in these reactions the form factor generally has a structure corresponding to much smaller masses than the mass of the exchanged particle. In other words, the whole dependence of the cross section on the propagator of the exchanged meson is masked by the more rapid fall-off of the empirical form factor.

The need for such drastic form factors in both pion and vector meson exchange processes causes concern as to the validity of the simple peripheral model. One can argue about whether $F(\Delta^2)$ given by Eq. (2) does or does not vary "unreasonably" rapidly in Δ^2. But when similar functions of Δ^2 are needed, independently of the supposed exchange, there is reason to look for other ways of testing and verifying the basic assumptions of the peripheral model, and even of alternative explanations of the peripheral nature of the collisions.

Another indication of difficulty with the OPE model with form factors is found in a comparison of the reactions, $NN \to NN^*$ and $\bar{N}N \to \bar{N}N^*$ (and $N\bar{N}^*$). The OPE model predicts that, apart from Pauli principle considerations, the cross sections for the nucleon–nucleon and antinucleon–nucleon processes should be the same. The comparisons have been made recently,[22–24] and while there seems to be some disagreement among the experiments, the antinucleon–nucleon results give much smaller cross sections and somewhat narrower angular distributions that predicted by the Ferrari–Selleri model, fitted to the nucleon–nucleon data. These differences between nucleon–nucleon and antinucleon–nucleon peripheral production reactions find a natural qualitative explanation in the absorptive model described in Sec. 5.

3. DECAY CORRELATIONS

In the discussion of the previous section, the quasi-two-body reactions have been treated as involving stable entities. In actual fact, one or both of the objects in the final state breaks up rapidly into several particles whose momenta are eventually observed or inferred. The angular distributions of decay of the resonances contain information about the production process, in a manner familiar in low-energy nuclear reactions where the angular distribution of photons from the de-excitation of the final nucleus bears on the mode of its formation.[25] Originally, the converse applied: an assumption about the production process was made [e.g., dominance of the OPE contribution of Fig. 5(b)], and properties of the resonance were inferred from the angular distribution of decay (e.g., from the $\cos^2\theta$ dependence of the π–π scattering cross section at the ρ-meson peak, the spin of the ρ can be deduced to be unity). But once the spin and parity of the resonance is known, the decay correlations lead back to the magnetic substate populations of the spin of the resonance; these in turn yield information on the production act. This gives hope that the dominance of a given exchange mechanism can be tested from the decay correlations, independently of the momentum-transfer distributions.

The choice of axes with respect to which the decay correlations are expressed is arbitrary, but it is often important to choose an appropriate set in order to maximize certain features. For peripheral collisions there is a natural choice that emphasizes the exchanged system. The operational definition of the axes is that in the rest frame of the resonance the z axis is taken parallel to the momentum of the incident particle as seen in that frame and the y axis is in the direction of the normal to the production plane. In terms of the general diagram of Fig. 5(a), with c as the resonance, the incident particle is a and the normal to the production plane is $\mathbf{n}=\hat{d}\times\hat{a}/|\hat{d}\times\hat{a}|$, where $\hat{d}$ and $\hat{a}$ are unit vectors in the direction of the momenta of particles d and a in the rest frame of c. The naturalness of the choice for the z axis is obvious when one notes that the three-momentum transfer, $\mathbf{e}=\mathbf{c}-\mathbf{a}$, is antiparallel to $\hat{a}$, the z axis, in the rest frame of c. The choice of the y axis is less important, but is made so that the azimuthal angle ϕ is equal to the well-known Treiman–Yang angle.[26]

The spin population of a resonance can be described by a Hermitian density matrix $\rho_{mm'}$, where m and m' are magnetic quantum numbers relative to the z axis specified above. Parity conservation in the production process relates elements of the density matrix as follows[27]:

$$\rho_{-m,-m'}=(-1)^{m-m'}\rho_{mm'}, \tag{3}$$

and reduces the number of real parameters from $(2J+1)^2$ to $(2J^2+2J+1)$ for J integral and $(\frac{1}{2})\times$

[22] O. Czyzewski, B. Escoubés, Y. Goldschmidt-Clermont, M. Guinea-Moorhead, T. Hofmokl, *et al.*, in *Proceeding 1963 Sienna Conference on Elementary Particles* (Italian Physical Society, Bologna, 1963), Vol. I, p. 271; in *Proceedings of the XIIth International Conference on High Energy Physics (Dubna, 1964)* (Atomizdat, Moscow, 1965), Abstract VII-65; and private communication.

[23] T. C. Bacon, H. W. K. Hopkins, D. K. Robinson, E. O. Salant, A. Engler, *et al.*, in *Proceedings of the XIIth International Conference on High Energy Physics (Dubna, 1964)* (Atomizdat, Moscow, 1965), Abstract VII-66 (BNL 8268).

[24] T. Ferbel, H. Krayhill, J. Johnson, J. Sandweiss, and H. Taft, in *Proceedings of the XIIth International Conference on High Energy Physics (Dubna, 1964)* (Atomizdat, Moscow, 1965), Abstract II-45.

[25] The literature on decay correlations in inelastic nuclear collisions is extensive; a representative sampling is G. R. Satchler, Proc. Phys. Soc. (London) **A68,** 1037 (1955); M. K. Bannerjee and C. A. Levinson, Ann. Phys. (N.Y.) **2,** 499 (1957); A. B. Clegg and G. R. Satchler, Nucl. Phys. **27,** 431 (1961); J. S. Blair and L. Wilets, Phys. Rev. **121,** 1493 (1961); K. K. McDaniels, D. L. Hendrie, R. H. Bassel, and G. R. Satchler, Phys. Letters **1,** 295 (1962); R. A. Lasalle, J. G. Cramer, and W. W. Eidson, Phys. Letters **5,** 170 (1963); J. G. Cramer and W. W. Eidson, Nucl. Phys. **55,** 593 (1964) and following experimental paper; D. R. Inglis, Phys. Letters **10,** 336 (1964). The paper by Clegg and Satchler bears the closest resemblance to the present work.

[26] J. D. Jackson, Nuovo Cimento **34,** 1644 (1964).

[27] K. Gottfried and J. D. Jackson, Nuovo Cimento **33,** 309 (1964); Phys. Letters **8,** 144 (1964).

$(2J+1)^2$ for J half-integral, not including the trace condition, $\mathrm{Tr}\,\rho=1$.

For a resonance with $J=1$ the density matrix can be written explicitly as

$$\rho=\begin{pmatrix} \rho_{11} & \rho_{10} & \rho_{1,-1} \\ \rho_{10}^* & \rho_{00} & -\rho_{10}^* \\ \rho_{1,-1} & -\rho_{10} & \rho_{11} \end{pmatrix} \tag{4}$$

with three real elements ($\rho_{11}, \rho_{00}, \rho_{1,-1}$) and one complex ($\rho_{10}$). The angular distribution of decay can be written down in a straightforward manner in terms of the elements of the density matrix. For the important example of a $J=1$ resonance decaying via a parity-conserving interaction into two spinless bosons (e.g., $\rho\to 2\pi$, $K^*\to K\pi$) the general angular distribution of the decay products is [27]

$$W(\theta,\phi)=(3/4\pi)\{\rho_{00}\cos^2\theta+\rho_{11}\sin^2\theta - \rho_{1,-1}\sin^2\theta\cos 2\phi-\sqrt{2}\,\mathrm{Re}\,\rho_{10}\sin 2\theta\cos\phi\}. \tag{5}$$

It is interesting to note that almost all of the density matrix (4) is determined by a measurement of $W(\theta,\phi)$; only $\mathrm{Im}\,\rho_{10}$ remains unknown.

For a resonance with $J=1$ decaying into three pseudoscalar mesons (e.g., $\omega^0\to\pi^+\pi^-\pi^0$) the distribution is still given by (5), but the angles (θ,ϕ) refer to the direction of the normal to the plane containing the three decay products.

An important group of baryonic resonances have $J=\frac{3}{2}$ and decay via strong interactions into a spinless boson and a baryon of spin $\frac{1}{2}$. For such resonances the density matrix is parameterized by eight real numbers and the general angular distribution of decay is[27]

$$W(\theta,\phi)=(3/4\pi)\{\rho_{33}\sin^2\theta+\rho_{11}(\tfrac{1}{3}+\cos^2\theta) - (2/\sqrt{3})\,\mathrm{Re}\,\rho_{3,-1}\sin^2\theta\cos 2\phi - (2/\sqrt{3})\,\mathrm{Re}\,\rho_{31}\sin 2\theta\cos\phi\}, \tag{6}$$

where the subscripts on the density matrix elements are $2m$ and $2m'$.

General decay correlations such as (5) and (6) have their form delimited by the type of exchange that is assumed to occur. In terms of the general diagram of Fig. 5(a) the systems a and e collide to form the resonant state c. The laws of angular momentum and parity can be used to study the problem of the population of the magnetic substates of the resonance.[28] Since the coordinate axes have been chosen so that a and e are moving parallel to the z axis, the orbital angular momenta involved cannot give rise to m or m' different from zero. Nonvanishing m and m' values can only come from the intrinsic spins of the systems a and e.

If the system e (i.e., the t-channel state) has angular momentum $J_e=0$, as occurs in the OPE model, for example, then the only nonvanishing density matrix elements will have m and m' values less than or equal to J_a. If particle a is a pseudoscalar meson, then only ρ_{00} will be different from zero; if a is a nucleon, the only nonvanishing elements of the density matrix will have $m, m'=\pm\frac{1}{2}$. This means that the vector meson and isobar decay correlations, (5) and (6), have very simple forms when spin-zero exchanges occur, namely $W(\theta,\phi)\sim\cos^2\theta$ for $J=1$ mesonic resonances and $(1+3\cos^2\theta)$ for $J=\frac{3}{2}$ baryonic resonances.

A striking contrast exists when a vector meson is formed from an incident pseudoscalar meson and a $J_e=1^-$ exchange. Parity conservation restricts the orbital angular momentum to odd values and angular momentum conservation requires $l=1$. The probability of populating a magnetic substate m is proportional to the Clebsch–Gordan coefficient, $\langle 1m\,|\,110m\rangle$, which vanishes for $m=0$. Thus the only nonvanishing elements in (4) are ρ_{11} and $\rho_{1,-1}$, and the decay correlation (5) takes the form, $W(\theta,\phi)\sim\sin^2\theta\ (a+b\cos 2\phi)$. Actually this result holds for a more general configuration in the t channel containing a linear combination of states with arbitrary angular momentum $J_e\geq 1$ and parity $(-1)^{J_e}$, but the most natural state within the framework of the peripheral model is a vector meson.

Decay correlations have been observed in a variety of reactions. For the two-pion system in the reaction $\pi^\pm p\to\pi^\pm\pi^0 p$ at incident energies of a few GeV the angular distribution is more or less isotropic in the azimuthal angle ϕ and has an $(a+b\cos^2\theta)$ variation in the polar angle for a two-pion invariant mass at the ρ-meson mass. Below and above the resonance position the angular distribution shows an asymmetry about 90° which changes sign in a manner appropriate for the interference of a resonant and a small nonresonant amplitude.[29] At resonance the angular distribution is described well by (5) with $\langle\rho_{00}\rangle\sim 0.6-0.8$ and $\langle\rho_{1,-1}\rangle$, $\langle\mathrm{Re}\,\rho_{10}\rangle$ small, quite consistent with pion exchange as the mechanism of production.

Similar evidence for pion exchange occurs in the reaction $K^+p\to K^*N^*$ at 1.96 GeV/c [30] and 3 GeV/c.[4] Here decay correlations for both K^* and N^* are observed. The K^* decay data are in accord with (5), with a small azimuthal variation and the predominance of the term, $\rho_{00}\cos^2\theta$. The analogous distribution (6) for the N^* decay products is dominated by the second term, as expected for pion exchange.

A very different circumstance occurs for the data on K^* production at 3 GeV/c shown in Figs. 1 and 3. The

[28] Some of the arguments involving orbital angular momentum and intrinsic spins used below are dubious without rather careful definitions for relativistic situations. A proper treatment using a partial wave decomposition in the t channel is given in Ref. 27.

[29] For simplicity we shall ignore these and other nonresonant effects. For the $\pi^+\pi^-$ system there is a forward–backward asymmetry which does not change sign across the resonance. This may arise from contributions from the $T=0$ and $T=2$ states, although the detailed energy dependence is rather hard to understand.

[30] W. Chinowsky, G. Goldhaber, S. Goldhaber, W. Lee, and T. O'Halloran, Phys. Rev. Letters **9**, 330 (1962); G. Goldhaber, W. Chinowsky, S. Goldhaber, W. Lee, and T. O'Halloran, Phys. Letters **6**, 62 (1963).

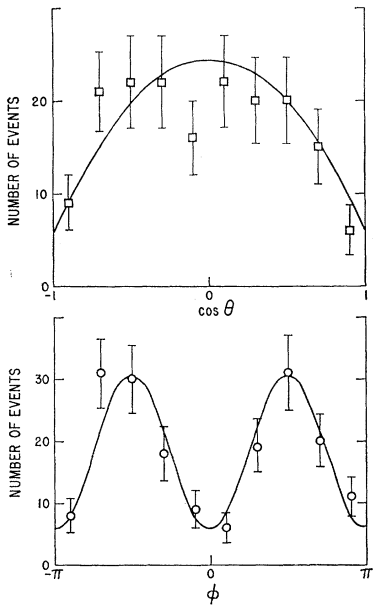

FIG. 7. Angular distributions in $\cos\theta$ and in ϕ for the decay products K^0 and π^+ from the resonance K^* produced in the reaction $K^+p\to K^*p$ at 3 GeV/c. The angular correlation variables (θ, ϕ) are defined in the text; the angle ϕ is the Treiman–Yang angle. The data are from Ref. 4.

decay distributions in $\cos\theta$ and ϕ are shown in Fig. 7. The $\cos\theta$ distribution is strongly $\sin^2\theta$ and the ϕ distribution shows striking oscillations. A detailed fitting with Eq. (5) yields the density-matrix elements, averaged over production angles, $\langle\rho_{00}\rangle=0.07\pm0.06$, $\langle\rho_{1,-1}\rangle=0.32\pm0.06$, $\langle\mathrm{Re}\ \rho_{10}\rangle=-0.10\pm0.05$.[4] These data thus give evidence for a large contribution from vector meson exchange, or at least exchanges other than that of a pion. Pion exchange does, of course, occur and with a known absolute rate (determined by the pion–nucleon coupling constant and the observed width of the K^*). But other exchanges are equally or more important. A detailed analysis of this reaction, including the behavior of the decay correlations as a function of momentum transfer is given in Sec. 6 after the peripheral model with absorption is described.

An interesting experiment has been performed recently[31] on the process $KN\to K^*N$ that throws light on the nature of the exchanged particles. K^+ mesons of momentum 2.3 GeV/c were incident on deuterium, and K^* formation in following reactions was studied:

$$K^+p(n)\to K^0\pi^+p(n) \qquad \text{(a)}$$

$$K^+n(p)\to K^0\pi^+n(p) \qquad \text{(b)}$$

$$K^+n(p)\to K^+\pi^-p(p). \qquad \text{(c)}$$

The spectator nucleon is indicated in parentheses on either side of the reaction. In reactions (a) and (b) the K^* system has the same charge as the incident K^+ meson, while in reaction (c) the charge of the K^* differs by one unit. In terms of the charge Q_{ex} of the exchanged system e in Fig. 5(a), reactions (a) and (b) involve $Q_{ex}=0$, while reaction (c) has $|Q_{ex}|=1$. For reactions (a) and (b) the exchanged system can therefore have isospin $T=0$ or $T=1$, but in reaction (c) can only have $T=1$. Pion exchange can occur in all three reactions, but of the vector mesons, ω, ϕ, and ρ can contribute to (a) and (b), while only the ρ meson can contribute to (c).

The various experimental distributions are shown in Fig. 8. To increase the statistics the two similar reactions, (a) and (b), have been combined. The upper histograms show the production angular distributions for $\Delta^2<20m_\pi^2$. The data indicate that reaction (c), with $|Q_{ex}|=1$, is more peripheral than the other and so might involve the exchange of a lighter particle. The decay correlations in the middle and lower parts of the figure bear this out. For $Q_{ex}=0$ the $\cos\theta$ distribution strongly resembles $\sin^2\theta$, in agreement with the data at 3 GeV/c shown in Fig. 7, while the corresponding distribution for $|Q_{ex}|=1$ looks very much like $\cos^2\theta$. The azimuthal distribution for $Q_{ex}=0$ is somewhat puzzling since it appears to have an oscillation of the form, $\cos 4\phi$, rather than $\cos 2\phi$, as given by (5). The $|Q_{ex}|=1$ distribution is consistent with isotropy.

These data are consistent with the interpretation that for $Q_{ex}=0$ a mixture of pion and vector meson exchange occurs and for $|Q_{ex}|=1$ only pion exchange. Thus the vector meson exchange contribution is con-

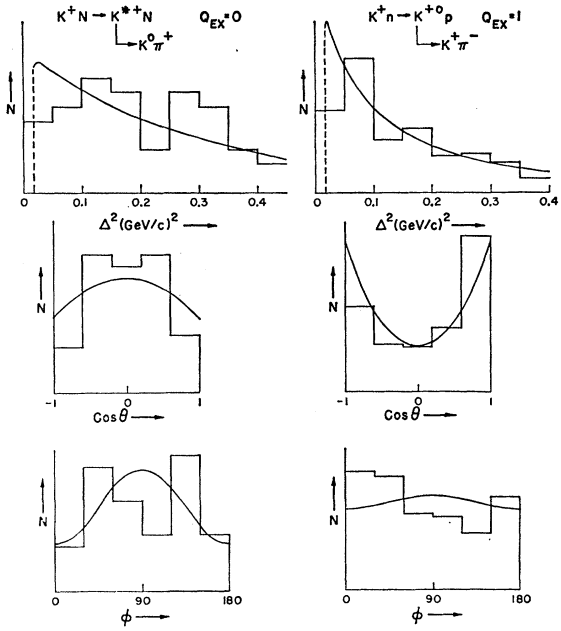

FIG. 8. Production angular distributions and decay correlations for K^* produced in K^+d collisions at 2.3 GeV/c. The data are from Ref. 31. The left hand set of histograms represent data with $Q_{ex}=0$ from the reactions $K^+p(n)\to K^0\pi^+p(n)$ and $K^+n(p)\to K^0\pi^+n(p)$; the right-hand set represent data with $|Q_{ex}|=1$ from the reaction $K^+n(p)\to K^+\pi^-p(p)$. The upper, center, and lower histograms give the angular (Δ^2) distribution of production, and the decay correlations in $\cos\theta$ and ϕ, respectively. The curves are calculated in the peripheral model with absorption, assuming pion and isoscalar vector meson exchanges.

[31] S. Goldhaber, I. Butterworth, G. Goldhaber, A. A. Hirata, J. A. Kadyk, *et al.*, in *Proceedings of the XIIth International Conference on High Energy Physics (Dubna, 1964)* (Atomizdat, Moscow, 1965), Abstract VIII-16 (UCRL-11465).

fined to the $T=0$ state (ω or ϕ). This conclusion had been reached tentatively by an indirect argument involving the reactions $KN\to K^*N$ and $KN\to K^*N^*$.[21] The fact that the exchange of ρ mesons does not seem to occur is in agreement with the ideas of Bronzan and Low[32] on the approximate conservation of a mesonic quantum number called amplitude parity. The curves in Fig. 8 are calculated with the peripheral model including absorption and are discussed briefly in Sec. 6.

It sometimes happens that the "natural" choice of axes and angles made above is not the best set for describing a decay correlation. The production of $J=\frac{3}{2}^+$ isobars in reactions such as $\pi N\to\pi N^*$ is an example. Here a specific dynamical assumption, the so-called ρ-meson–photon analogy of Stodolsky and Sakurai,[20] implies that angular correlations with respect to the normal $\mathbf{n}$ to the production plane are simple and characteristic. Figure 9 shows the relevant diagrams. Conservation of parity at the upper vertex in Fig. 9(a) forces the exchanged system to have angular momentum J_e and parity $(-1)^{J_e}$, while isospin conservation at the lower vertex requires the exchanged system to have $T=1$ or $T=2$. The ρ meson is an obvious candidate. The lower vertex in Fig. 9(a) is closely similar to the photoproduction vertex in Fig. 9(b) since it is the isovector part of the photon that is effective in formation of the isobar. Furthermore it is known that the isovector part of the γNN vertex (the electromagnetic form factor) is dominated by the contribution from the ρ meson. Thus it is natural to assume that the coupling of the ρ meson to the nucleon–isobar system in Fig. 9(a) is proportional to the photoproduction diagram of Fig. 9(b). This is the basis of the Stodolsky–Sakurai model.

The decay correlations expected follow from the empirical fact that the photoproduction reaction proceeds via the absorption of a magnetic-dipole photon. The photoproduction matrix element can thus be written symbolically as

$$\langle N^* \mid H_{\rm em} \mid N\rangle \simeq \langle N^* \mid \boldsymbol{\mu}_{\rm op}\cdot\mathbf{B} \mid N\rangle,$$

where the magnetic field $\mathbf{B}\sim\mathbf{k}\times\boldsymbol{\varepsilon}$, and $\boldsymbol{\mu}_{\rm op}$ is the effective magnetic-moment operator. With the ρ-meson–photon analogy, the lower vertex in Fig. 9(a) is proportional to this photoproduction amplitude with the "magnetic field" of the ρ meson replacing the ordinary magnetic field. Thus the vertex factor is proportional to

$$\langle N^* \mid \boldsymbol{\mu}_{\rm op}\cdot(\boldsymbol{\Delta}\times\boldsymbol{\varepsilon}_\rho) \mid N\rangle,$$

where $\boldsymbol{\Delta}$ is the momentum of the virtual ρ-meson and $\boldsymbol{\varepsilon}_\rho$ is its polarization vector. The upper vertex in Fig. 9(a) can be thought of as the decay vertex of the ρ meson. Since the decay vertex is proportional to $\boldsymbol{\varepsilon}_\rho\cdot(\mathbf{p}_+ + \mathbf{p}_0)$, where $\mathbf{p}_+$ and $\mathbf{p}_0$ are the momenta of the pions, the polarization vector $\boldsymbol{\varepsilon}_\rho$ of the virtual ρ meson

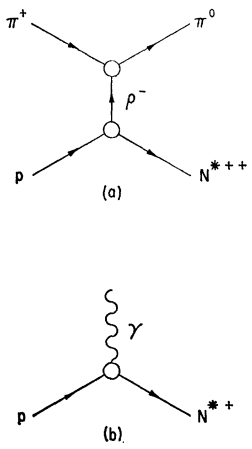

FIG. 9. (a) Diagram for the reaction $\pi^+p\to\pi^0N^{*++}$ with ρ exchange. (b) Diagram for photoproduction in the neighborhood of the (3, 3) resonance.

must lie in the production plane. Consequently the only effective component of $\boldsymbol{\mu}_{\rm op}$ in the matrix element is that along the normal to the production plane. By the well-known selection rules for a vector operator, this implies that the magnetic quantum numbers in the initial and final states are the same when expressed relative to the normal. The only magnetic substates of the N^* that are populated are thus $m=\pm\frac{1}{2}$. This leads to a decay distribution of the form, $1+3\cos^2\theta_n$, where θ_n is the polar angle expressed relative to the normal.

The Stodolsky–Sakurai prediction for the decay distribution of isobars has been verified in its essentials in several experiments with incident pions and K-mesons. The data shown in Figs. 1 and 4 for the reaction $K^+p\to K^0N^{*++}$ at 3 GeV/c yield decay distributions relative to the normal of the form, $1+a\cos^2\theta_n$, with $a\simeq 2.4$. Similar results are found for $\pi^+p\to\pi^0N^{*++}$ at 3.54 GeV/c.[33]

The angular distribution (6) can, of course, be transformed into a distribution with respect to the normal to the production plane. With spherical angles (θ_n, Φ_n) relative to the normal, the general decay distribution for a $J=\frac{3}{2}$ system going into a spinless boson and a spin-$\frac{1}{2}$ fermion is

$$\begin{aligned} W(\theta_n,\Phi_n) = (3/4\pi)\{&\tfrac{1}{2}(\rho'_{33}+\rho'_{-3,-3})\sin^2\theta_n \\ &+\tfrac{1}{2}(\rho'_{11}+\rho'_{-1,-1})(\tfrac{1}{3}+\cos^2\theta_n) \\ &-(1/\sqrt{3})\,\mathrm{Re}\,(\rho'_{3,-1}+\rho'_{-3,1})\sin^2\theta_n\cos 2\Phi_n \\ &+(1/\sqrt{3})\,\mathrm{Im}\,(\rho'_{3,-1}-\rho'_{-3,1})\sin^2\theta_n\sin 2\Phi_n\}, \quad (7) \end{aligned}$$

where $\rho'_{2m,2m'}$ are the elements of the resonance's spin-density matrix relative to the normal [cf., Eq. (42) of Ref. 27]. If the azimuthal angle Φ_n is defined relative to the momentum of incident baryon, as seen in the resonance's rest frame as x axis [the z axis for the "natural" system used in (6)], the density-matrix

[32] J. B. Bronzan and F. E. Low, Phys. Rev. Letters **12**, 522 (1964).

[33] M. Abolins, D. D. Carmony, D. -N. Hoa, R. L. Lander, C. Rindfleisch *et al.*, Phys. Rev. **136**, B195 (1964).

elements appearing in (7) are related to those in (6) through

$$\tfrac{1}{2}(\rho'_{33}+\rho'_{-3,-3})=\tfrac{1}{4}(\tfrac{3}{2}-2\rho_{33}-2\sqrt{3}\ \mathrm{Re}\ \rho_{3,-1}),$$

$$\tfrac{1}{2}(\rho'_{11}+\rho'_{-1,-1})=\tfrac{1}{4}(\tfrac{1}{2}+2\rho_{33}+2\sqrt{3}\ \mathrm{Re}\ \rho_{3,-1}),$$

$$(1/\sqrt{3})\ \mathrm{Re}\ (\rho'_{3,-1}+\rho'_{-3,1})=-\tfrac{1}{4}+\rho_{33}-(1/\sqrt{3})\ \mathrm{Re}\ \rho_{3,-1},$$

$$(1/\sqrt{3})\ \mathrm{Im}\ (\rho'_{3,-1}-\rho'_{-3,1})=-(2/\sqrt{3})\ \mathrm{Re}\ \rho_{31}, \qquad (8)$$

and similar inverse relations. The Stodolsky–Sakurai model gives only ρ'_{11} and $\rho'_{-1,-1}$ nonvanishing in (7), corresponding to $\rho_{33}=\frac{3}{8}=0.375$, $\mathrm{Re}\ \rho_{3,-1}=\sqrt{3}/8=0.216$, and $\mathrm{Re}\ \rho_{31}=0$. For the data in Fig. 4, the average values of these parameters are found to be $\langle\rho_{33}\rangle=0.28\pm0.06$, $\langle\mathrm{Re}\ \rho_{3,-1}\rangle=0.21\pm0.05$, $\langle\mathrm{Re}\ \rho_{31}\rangle=0.04\pm0.05$,[4] in generally good agreement with the model.

The examples of decay correlations described in the previous paragraphs indicate that peripheral production reactions often involve the exchange of specific angular momenta, or in terms of light particles, the exchange of pseudoscalar or vector mesons. These data thus provide justification for the OPE model and its generalizations to include vector meson exchange, in spite of the doubts raised in Sec. 2 by the need to use drastic form factors to fit the momentum transfer distributions.

4. ABSORPTIVE EFFECTS AS A SOURCE OF COLLIMATION

The discussion of the previous two sections poses the following puzzle concerning quasi-two-body peripheral collisions: On the one hand the decay correlation data from various reactions are simply understood on the basis of the preponderance of a definite spin and parity state for the exchanged system, sometimes $T=1$, $J=0^-$ (pion) exchange, sometimes $T=0$, $J=1^-$ (ω or ϕ) exchange, and so on. But on the other hand, the momentum-transfer distributions for all reactions are very strongly peaked at small Δ^2, with angular spreads that are largely independent of the type of exchange occurring and bearing little or no relation to the mass of the possible exchanged particle. For both pion and vector meson exchanges the observed momentum-transfer distributions are grossly overly peripheral in comparison with simple theory.

Ferrari and Selleri[16] and others[21] have suggested form factors as the solution to the problem of the momentum transfer dependence, but, as has already been discussed at the end of Sec. 2, the *ad hoc* nature of this assumption and the radical behavior of the form factors needed casts it in serious doubt. A description of the exchanged systems as Regge poles was at one time suggested[27] as a mechanism for maintaining the decay correlations while providing a steep and relatively universal dependence in momentum transfer. But Regge-pole exchange is somewhat unpopular nowadays and is probably rather naive, at least at energies in the few GeV range. The main virtue of Regge-pole exchange is that it provides a link between elastic scattering and the quasi-two-body production reactions. Such a connection had in fact been noted by various experimental groups who compared the slopes of their production cross sections with the slope of the elastic scattering diffraction peak.

This last remark contains the germ of the most probable explanation of the peripheral nature of quasi-two-body reactions. The collimation observed in elastic diffraction scattering arises in the crudest sense from the existence of a strongly absorbing region of finite extent—the forward elastic peak is "shadow" scattering. It seems eminently reasonable that these same absorptive effects operate in quasi-two-body reactions and produce a similar forward peaking.

In the language of reaction theory, there exist numerous competing open channels. A particular quasi-two-body production channel usually accounts for only a small fraction of the total inelastic cross section, and many of the other channels represent more complex final states involving numerous and/or uncorrelated particles. These more complicated reactions are expected on simple intuitive grounds to be initiated in the more violent collisions with large momentum transfers, or equivalently at small impact parameters. This means that the close collisions are not effective in causing the relatively simple quasi-two-body reactions. There is a qualitatively analogous situation in the stripping and pick-up reactions of low energy nuclear physics where collisions involving deep penetration into the nucleus do not contribute to the direct reactions.

The existence of competing channels can be expected to reduce the low partial-wave reaction amplitudes below the values given by the simple peripheral model, while leaving the higher partial waves essentially unchanged. The results of this damping of the low partial waves are (a) a reduction of the reaction cross section, (b) important modifications of the angular distribution, and (c) alteration of the decay correlations. As will be seen from the detailed calculations described below, all of these changes are such as to give general agreement with experiment.

Although earlier considerations of the absorptive effects of many open channels exist,[34,35] the essentials of the present model are first found in the work of Sopkovich[36] who applied what is basically the distorted-wave Born approximation to the two-body reaction $\bar{p}p\to\bar{\Lambda}\Lambda$. A simpler model was proposed by Dar, Kugler, Dothan, and Nussinov,[37] who suggested that the peripheral reactions arose from collisions of a definite

[34] B. T. Feld, Angular Distribution in Nucleon-Nucleon "Quasi-Elastic Diffraction" Scattering (unpublished), CERN Report 1114 Th. 178 (1961). The effects of N^* spin were included in an approximate way by Feld in a subsequent unpublished CERN report 1700/Th. 193 (1961).

[35] M. Baker and R. Blankenbecler, Phys. Rev. **128,** 415 (1962).

[36] N. J. Sopkovich, Nuovo Cimento **26,** 186 (1962).

[37] A. Dar, M. Kugler, Y. Dothan, and S. Nussinov, Phys. Rev. Letters **12,** 82 (1964).

impact parameter, inside of which the collisions were all complex and highly inelastic. This model was later altered so that those parts of the one-meson exchange amplitude corresponding to collisions at impact parameters greater than some minimum were effective in the reaction.[38] In this form it resembles the Born approximation with a sharp cutoff in configuration space. More realistic descriptions of the absorptive effects have been given by Durand and Chiu,[39] Ross and Shaw,[40] and Gottfried and Jackson.[41] Spin effects are shown in Ref. 41 to be of great importance, not only for the decay correlations but also for the angular distributions of production.[42].

At the present time a large number of quasi-two-body reactions have been studied using the peripheral model with absorptive effects. These include $\pi N \to \rho N$;[40,41,43–45] $\pi^+ n \to \omega p$;[45] $\bar{N}N \to \bar{N}N^*$, $\bar{N}^*N$, $\bar{N}^*N^*$;[39,46] $KN \to K^*N$, KN^*, K^*N^* and the corresponding reactions with $\bar{K}$; $K^- p \to \pi Y^*$;[45] $\pi N \to \pi N^*$, ρN^*.[44,45] In the following paragraphs the formalism and some of the results of Refs. 41, 44, and 45 will be described.

5. PERIPHERAL MODEL WITH ABSORPTION

In the distorted-wave Born approximation of low-energy nuclear physics the transition amplitude T_{fi} is approximated by the matrix element

$$T_{fi} \simeq \langle \Psi_f^{(-)} \mid V \mid \Psi_i^{(+)} \rangle, \tag{9}$$

where V is the interaction causing the transition (e.g., the two-body force between nucleons), $\Psi_i^{(+)}$ is the correct wave function of the system in the initial state in the absence of V, and $\Psi_f^{(-)}$ is the corresponding wave function in the final state. The wave functions $\Psi^{(\pm)}$ are customarily approximated by the wave functions of an optical-model potential whose imaginary part simulates the absorptive effects of the many competing channels. The particular optical-model potential employed is usually one which gives an adequate representation of the elastic scattering at the same energy. In reactions at high energies where the wavelengths are short compared to the characteristic lengths of the forces simplifications occur that allow elimination of the optical-model potential. The absorptive effects in an inelastic process can be expressed directly

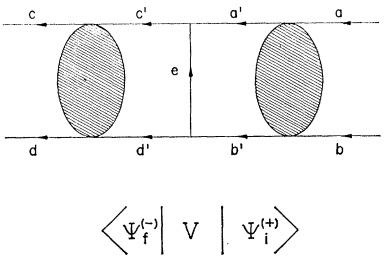

FIG. 10. Schematic representation of the distorted-wave Born approximation at high energies. The matrix element involving distorted wave functions in the intial and final states can be expressed in terms of the one-particle-exchange diagram modified by elastic scattering in the initial and final states (represented by the shaded blobs).

in terms of elastic scattering data. Figure 10 indicates schematically the low- and high-energy situations. For high energies the one-particle-exchange diagram represents the interaction potential V. The shaded blobs on either side indicate elastic scattering in the initial and final states. In the high-energy limit these are on-the-mass-shell scattering and so can be expressed in terms of the elastic-scattering phase shifts.

The small-angle elastic scattering of all particles at energies above 1 or 2 GeV shows a diffraction pattern with a roughly exponential decrease with increasing momentum transfer (Δ^2). Furthermore, the data extrapolate within errors to the optical theorem point at zero degrees, implying that the scattering amplitude is mainly imaginary, at least at small angles.[47] To the extent that the exponential shape holds and the real part of the amplitude can be neglected, the elastic-scattering cross section can then be written as

$$d\sigma/d\Delta^2 \simeq (\sigma^2_{\text{total}}/16\pi) \exp(-A\Delta^2). \tag{10}$$

The scattering at small angles is dominated by transitions involving no change in the spin orientations (helicities) of the particles since the spin–flip amplitudes vanish in the forward direction. There the elastic scattering can be described by a scalar amplitude $f_{\text{el}}(\theta)$. In terms of an impact parameter representation (appropriate when many partial waves contribute) $f_{\text{el}}(\theta)$ is

$$f_{\text{el}}(\theta) \simeq -iq \int_0^\infty dbbJ_0(\Delta b)\{\exp[2i\delta(b)]-1\}, \tag{11}$$

where q is the center-of-mass momentum, Δ is the momentum transfer [$\Delta^2 = 4q^2 \sin^2(\theta/2)$], and $\delta(b)$ is a complex phase shift corresponding to δ_l with the identification $l = qb$. The exponential behavior (10) of the cross section and the assumption that $f_{\text{el}}(\theta)$ is purely imaginary implies that $\exp[2i\delta(b)]$ is real [i.e., $\delta(b)$ is purely imaginary], and has the approxi-

[38] A. Dar and W. Tobocman, Phys. Rev. Letters **12**, 511 (1964); A. Dar, **13**, 91 (1964).
[39] L. Durand and Y. T. Chiu, Phys. Rev. Letters **12**, 399 (1964); **13**, 45E (1964).
[40] M. H. Ross and G. L. Shaw, Phys. Rev. Letters **12**, 627 (1964).
[41] K. Gottfried and J. D. Jackson, Nuovo Cimento **34**, 735 (1964).
[42] This point has been recognized by Durand and Chiu (see the errata to Ref. 39 and also Ref. 43).
[43] L. Durand, paper presented at the Conference on Particle and High Energy Physics, Boulder, Colorado, 1964 (unpublished);
[44] K. Gottfried, J. D. Jackson, and B. Svensson in *Proceedings of the XIIth International Conference on High Energy Physics (Dubna, 1964)* (Atomizdat, Moscow, 1965), Abstract V-5.
[45] J. D. Jackson, J. T. Donohue, K. Gottfried, R. Keyser, and B. E. Y. Svensson, Phys. Rev. (to be published).
[46] L. Durand and Y. T. Chiu, Phys. Rev. (to be published).

[47] There is some recent evidence from Brookhaven and CERN that, contrary to previous notions, there may be a sizable real part (as much as 30–40% of the imaginary part). The calculations described here do not include this possibility, but the effects of a real part of the elastic amplitude are being investigated.

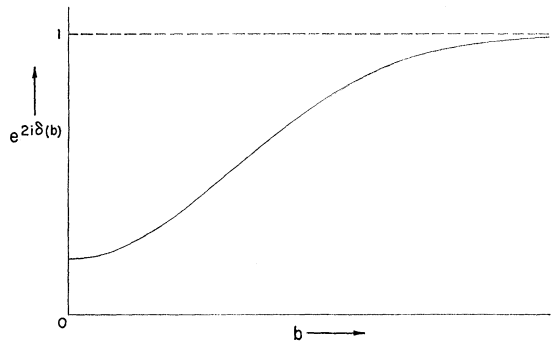

FIG. 11. Elastic-scattering phase factor exp $[2i\delta(b)]$ as a function of impact parameter. In the approximation described in the text, the phase shift $\delta(b)$ is purely imaginary and the function shown represents a "grey" absorption region with a Gaussian shape.

mate form

$$\exp[2i\delta(b)]\simeq 1-(\sigma_{\text{total}}/4\pi A)e^{-b^2/2A}. \quad (12)$$

For consistency, there is the requirement,

$$(\sigma_{\text{total}}/4\pi A)\leq 1,$$

or if (10) is taken to hold at all angles, $\sigma_{\text{el}}\leq\frac{1}{4}\sigma_{\text{total}}$. Fits to various data show that the coefficient $(\sigma_{\text{total}}/4\pi A)$ is of the order of 0.7–1.0, corresponding to complete or almost complete absorption of the s wave and other low partial waves, as indicated in Fig. 11.

The derivation of the high-energy version of the distorted-wave Born approximation (9) is discussed in Refs. 36, 41, and 43; only the main results will be presented here.[48] In the helicity formalism of Jacob and Wick[49] a transition amplitude for the reaction $ab\to cd$ can be expanded in angular momentum states as

$$\langle\lambda_c\lambda_d\mid T\mid\lambda_a\lambda_b\rangle=\sum_j(j+\tfrac{1}{2})\langle\lambda_c\lambda_d\mid T_j\mid\lambda_a\lambda_b\rangle d_{\lambda\mu}{}^j(\theta), \quad (13)$$

where λ_a, λ_b, λ_c, λ_d are the helicities of particles a, b, c, d, $\lambda=\lambda_a-\lambda_b$, $\mu=\lambda_c-\lambda_d$, and the $d_{\lambda\mu}{}^j(\theta)$ are the representations of the rotation group of dimension $(2j+1)$. In the limit of large j and small angles the rotational functions can be approximated by

$$d_{\lambda\mu}{}^j(\theta)\simeq J_n((2j+1)\sin(\theta/2)),$$

where $J_n(x)$ is the Bessel function of the first kind of order n, and $n=\mu-\lambda$. This is a generalization of the familiar result, $P_l(\cos\theta)\simeq J_0((2l+1)\sin(\theta/2))$. With this approximation, (13) can be converted into an impact parameter representation akin to (11):

$$\langle\lambda_c\lambda_d\mid T\mid\lambda_a\lambda_b\rangle\simeq\int_{x_{\min}}^{\infty}dxx\langle\lambda_c\lambda_d\mid T(x)\mid\lambda_a\lambda_b\rangle J_n(\omega x). \quad (14)$$

In (14), x represents $(j+\frac{1}{2})$, $x_{\min}$ is the smallest j value allowed in the sum (13), and $\omega=2\sin(\theta/2)$.

The reaction $ab\to cd$ is described by $\frac{1}{2}(2j_a+1)\times(2j_b+1)(2j_c+1)(2j_d+1)$ different helicity amplitudes. Each of the amplitudes corresponding to the one-particle-exchange diagram of Fig. 5(a) can be written in the form of (13) or (14) with an explicit expression for $\langle\lambda_c\lambda_d\mid T_j\mid\lambda_a\lambda_b\rangle$ or $\langle\lambda_c\lambda_d\mid T(x)\mid\lambda_a\lambda_b\rangle$. If these projections of the one-particle-exchange amplitude are denoted by a superscript B, then the high-energy equivalent of (9) is obtained by writing in (14),

$$\langle\lambda_c\lambda_d\mid T(x)\mid\lambda_a\lambda_b\rangle\simeq\exp[i\delta_{cd}(x)]\times\langle\lambda_c\lambda_d\mid T^{(B)}(x)\mid\lambda_a\lambda_b\rangle\exp[i\delta_{ab}(x)], \quad (15)$$

where $\delta_{ab}(x)$ and $\delta_{cd}(x)$ are the elastic-scattering phase shifts for the initial and final states, respectively (see Fig. 10). Equation (15) shows explicitly that the absorptive effects reduce the low partial waves below the one-particle-exchange amplitude.

An important observation must be made about the derivation of (15). It has been assumed that the initial and final-state interactions involve only nonhelicity changing scattering represented by (11). Thus the helicity state populations of the particles a', b', c', d' in Fig. 10 are the same as a, b, c, d for a given impact parameter. The helicity populations are altered from the one-particle-exchange amplitude only through the varying absorptive effects at different impact parameters.

If the final-state scattering were known, the model based on (15) would involve no free parameters since the absorptive factors could be read off from (12) or equivalent representations of the observed elastic-scattering data. Unfortunately the final-state partners are objects such as K^* and N^*, whose elastic scattering is unknown. Thus a simplifying ansatz must be made in order to proceed. One possibility is to assume that the final-state scattering is the same as the initial scattering. This was done in the early computations.[41,44] But a somewhat more reasonable and allowable approach is to assume a structure like (12) for the final state with a somewhat larger and more absorbing region (Fig. 11) than occurs in the known initial-state scattering.[45] For fixed initial-state parameters it turns out that the calculated cross sections are often not extremely sensitive to the final-state parameters (see Fig. 13 for one example).

It will be seen in the examples presented below that one-meson-exchange model has considerable success in

[48] None of the derivations can be said to be satisfactory and there are some ambiguities. Ross and Shaw (Ref. 40), for example, arrive at a somewhat different result than those of Refs. 36, 41, and 43. R. Omnes [Phys. Rev. **137**, B649 (1965)] has made an attempt to derive the basic results on rather general grounds. E. J. Squires [Nuovo Cimento **34**, 1328 (1964)] has also given a derivation based on a model using the multichannel N/D equations. A related, dispersion theory discussion has been presented recently by J. S. Ball and W. R. Frazer [Phys. Rev. Letters **14**, 746 (1965)].

[49] M. Jacob and G. C. Wick, Ann. Phys. (N. Y.) **7**, 404 (1959).

fitting the very peripheral production cross sections discussed in Sec. 2. But it was noted there that the OPE model with form factors achieved similar successes. The question arises as to whether the two models can be distinguished experimentally. Study of the preceding development shows that, to the extent that the elastic scattering (in initial and final states) does not change as a function of incident momentum, the overall effect of absorption can be expressed as a modification of the simple one-meson-exchange cross section by a function of Δ^2 alone, and hence cannot be distinguished experimentally from an energy-independent form factor. Considering the present accuracy of the production data it seems difficult to verify which hypothesis is more correct from the Δ^2 distributions alone, although the K^+, p, and $\bar{p}$ elastic scattering parameters vary sufficiently with energy that differences do occur.

Another method of discriminating between the two models is the study of corresponding peripheral reactions produced by particles and antiparticles. The comparison of isobar production by nucleons and antinucleons,[22–24] mentioned at the end of Sec. 2, can be understood readily on the basis of the absorptive model. At energies of a few GeV the antinucleon–nucleon total cross section is larger and the elastic diffraction peak is narrower than those for nucleons, an undoubted reflection of the many more highly inelastic channels available to the $\bar{N}N$ system. The absorptive region of Fig. 11 is "blacker" and larger for $\bar{N}N$ than for NN. This will inevitably mean that the $\bar{N}N$ quasi-two-body reaction cross sections will be smaller and more collimated than the corresponding NN cross sections, as is indeed observed.

Evidence in favor of form factors as the dominant mechanism for producing collimation can perhaps be found in the marked similarity in the differential cross section and decay correlations found for $K^+p\to K^*p$[4] and $K^-p\to\bar{K}^*p$[50] at 3 GeV/c, in spite of the rather different elastic scattering of K^+ and K^- at this energy. But within the errors of the experiments the absorptive model manages to give a satisfactory fit to both sets of data.[45]

Decay correlations are perhaps the best place to discriminate between the two models. The peripheral model with form factors predicts the same decay correlations at all Δ^2 (unless there is a superposition of two or more types of exchange with different dependences on Δ^2), while the peripheral model with absorption gives a variation of the decay parameters with Δ^2. Examples will be discussed below.

6. EXAMPLES

Calculations based on the model described in Sec. 5 have been programmed at CERN for the following reactions[45]:

$$PB(P' \text{ and } V')VB', \tag{16}$$

$$PB(V)P'B^*, \tag{17}$$

$$PB(P' \text{ and } V')VB^*, \tag{18}$$

where the letters P, V, B, B^* stand for pseudoscalar mesons, vector mesons, baryons, and $J=\frac{3}{2}^+$ baryon isobars, respectively. The initial state is on the left, the exchanged particles are in the parentheses, and the final state is on the right. For a given choice of masses, coupling constants, incident momentum, and absorption parameters in the initial and final states [σ_{total} and A in (12)], the differential cross section of production and the density matrix elements $\rho_{mm'}$ of each resonance are calculated as functions of momentum transfer. Unless otherwise indicated, in the examples discussed below the final-state scattering parameters are standardized to give *total* absorption of the lowest partial wave and to have a Gaussian region of absorption with a projected area 33% larger than the initial state. In the numerical calculations the representation of the absorptive effects actually employed in (15) is

$$\exp i(\delta_{cd}+\delta_{ab}) = [(1-C_2\exp[-\gamma_2(x-\tfrac{1}{2})^2]) \times (1-C_1\exp[-\gamma_1(x-\tfrac{1}{2})^2])]^{\frac{1}{2}}, \tag{19}$$

where C_1, C_2 are the amounts by which the lowest partial waves are absorbed in the initial and final states, respectively. The parameter γ_i is related to the slope factor A_i in (10) and (12) through $2\gamma_i A_i q_i^2=1$, where q_i is the center-of-mass momentum in the initial or final state. The choice of $(x-\frac{1}{2})$ instead of x in the exponentials is somewhat arbitrary, but is an attempt to relate the absorption to the orbital rather than the total angular momentum [note that in reactions (16)–(18) $j_{\min}=\frac{1}{2}$]. The parameters γ_1 and C_1 are taken from elastic-scattering data for the initial state. The "standard" choice mentioned above has $C_2=1$ and $\gamma_2=0.75\gamma_1$.

$\pi N(\pi)\rho N$

Much experimental data exist on ρ-meson production with both positive and negative pions at incident momenta ranging from 1.59 to 8 GeV/c or more. Theoretical results already exist in the literature.[40,41] Another example is shown in Fig. 6, for 2.75-GeV/c positive pions. The calculated curve, reaction (16) with only pion exchange, is in reasonable agreement with experiment, but cannot be preferred over the OPE model with a form factor. The calculated decay correlations, with $\langle\rho_{00}\rangle\sim 0.7$, are in accord with preliminary analysis of the data.

From 1.6 to 8 GeV/c the results calculated assuming only pion exchange are in good agreement with existing data on total cross section, angular distribution of production and decay correlations. There is, at present, no positive evidence for ω exchange, as might be ex-

[50] R. Barloutaud, A. Leveque, C. Louedec, J. Meyer, P. Schlein, *et al.*, in *Proceedings of the XIIth International Conference on High Energy Physics (Dubna, 1964)* (Atomizdat, Moscow, 1965), Abstract VIII-34.

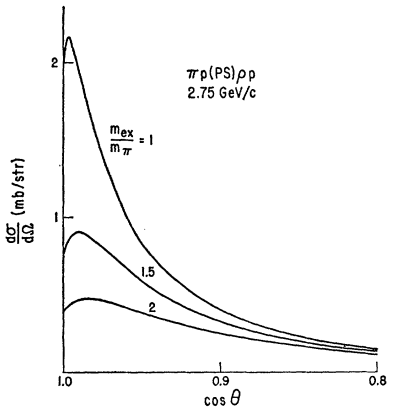

FIG. 12. Differential cross section for the reaction $\pi p(\pi)\rho p$ at 2.75 GeV/c, calculated with the OPE model including absorptive effects for various masses of the exchanged "pion." The different mass values are indicated on the curves. The upper curve agrees with experiment and is shown in Fig. 6.

pected from the supposed existence of a $\pi\rho\omega$ coupling.[51]

A point which might be noted in passing is that, although the absorption of low partial waves produces a marked collimation which depends largely on the elastic scattering, the mass of the exchanged particle still influences the shape of the angular distribution. This is illustrated in Fig. 12 where ρ-meson production at 2.75 GeV/c has been calculated with various masses for the exchanged pseudoscalar meson. The upper curve is that shown in Fig. 6 and agrees with experiment. It is seen that a factor of 1.5 increase in the mass of the exchanged "pion" is sufficient to cause gross disagreement with observation.

$\pi^+\mathrm{p}(\pi)\rho\mathrm{N}^*$

The presence of both ρ and N^* in the four-particle final-state $\pi^+p\to\pi^+\pi^-\pi^+p$ gives an example of reaction (18). A comparison of theory and experiment is given in Figs. 13 and 14. The angular distribution of production is shown in Fig. 13. The histogram represents the data at 4 GeV/c of the ABBBHLM collaboration.[10] In the theoretical calculations the finite widths of the ρ and N^* are ignored. Consequently there is a sharp theoretical lower limit to Δ^2, not present in the experimental data. In Fig. 13, to facilitate comparison of theory and experiment, the dashed rectangle next to this lower limit includes the area of those Δ^2 intervals below the theoretical minimum.

The various curves in Fig. 13, all giving reasonably good fits to the Δ^2 distribution, illustrate the effects of changing the final state scattering parameters in (19). The scattering of ρ mesons and the N^* isobar is probably represented only very approximately by (10)–(12), but presumably can be described crudely by a much blacker and larger absorbing region than π–N scattering. Thus $C_2\simeq 1$ and $\gamma_1\simeq\frac{1}{2}\gamma_1$ or even less are plausible choices in (19). One sees from Fig. 13 that a fairly wide variation in the values of C_2 and γ_2 does not produce qualitatively different features in the Δ^2 distribution.

The decay parameters for both the ρ meson and the isobar are shown in Fig. 14 as functions of Δ^2. The theoretical values are completely insensitive to the variations in the final-state scattering parameters of Fig. 13. Preliminary experimental values, which are averages over all Δ^2, are plotted arbitrarily at the average value of Δ^2 observed in the production angular distribution of Fig. 13. The agreement between theory and experiment is better than one has any right to expect. The calculated values of the density-matrix elements are close to those of the unmodified OPE model ($\rho_{00}=1$ for the ρ meson, $\rho_{11}=0.5$ for the isobar, all other $\rho_{mm'}=0$) at small Δ^2, but depart progressively with increasing Δ^2.

Two observations should be made here. One is that the experimental total cross section for this reaction at 4 GeV/c is estimated to be of the order of 1 mb or less, whereas the theoretical cross sections shown in Fig. 13 are all about 2.0–2.4 mb. Thus the one-meson-exchange model with absorption, while in reasonable accord with the shape of the angular distribution of production and the decay correlations, does not fit the absolute cross section at 4 GeV/c. At 8 GeV/c the situation is better; the theoretical cross section is 1.0 mb and the experimental value is 0.8–1.0 mb.[11] The other observation is that at 3.65 GeV/c there appear

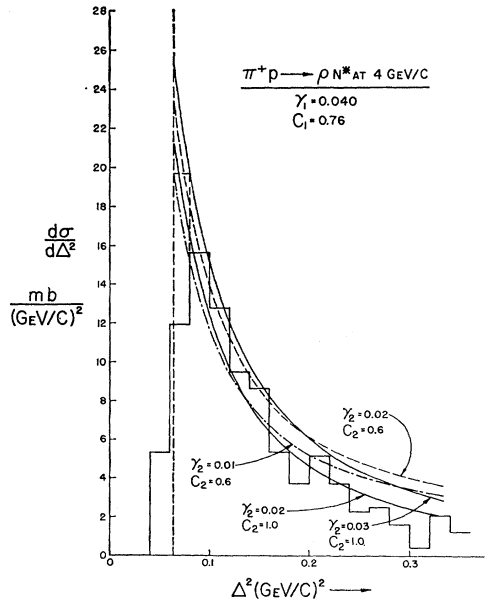

FIG. 13. Differential cross section for the reaction $\pi^+p(\pi)$ ρ^0N^{*++} at 4 GeV/c. The histogram represents the preliminary data of Ref. 10 with arbitrary normalization. The various theoretical curves differ by the final state scattering parameters used in (19). The inital-state parameters are $C_1=0.76$, $\gamma_1=0.040$.

[51] M. Gell-Mann, D. Sharp, and W. G. Wagner, Phys. Rev. Letters **8**, 261 (1962).

to be fairly strong *combined* decay correlation effects for the ρ and N^*.[52] In the simple OPE model such effects cannot occur because the exchanged particle has zero spin. But the presence of absorption alters this null result and gives combined correlations in general agreement with the data.[45]

$K^+p(\pi$ and $V)K^{*+}p$

The K^* production reaction $KN \to K^*N$, already discussed in Secs. 2 and 3, is an interesting example of reaction (16). It is pointed out in Sec. 3 that the decay correlation data of Fig. 7 implied a predominance of $J=1^-$ exchange, in contrast to ρ production. Since the pion-exchange diagram is fixed in absolute scale [in Fig. 5(a) the coupling at the upper vertex is related to the K^* width for decay into $K\pi$, while that for the lower vertex is given by the pion–nucleon coupling strength],[53] there is the question of whether the observed cross section is large enough to accommodate the necessary amount of vector exchange. A partial answer to this question is found in Fig. 15 where the dashed curve gives the result of the OPE model with absorption in comparison with the data at 3 GeV/c from Fig. 3. Pion exchange alone is too small and too peripheral.

The nature and strength of the vector exchange responsible for the angular distribution of production and the decay correlations of Fig. 7 are relatively closely delineated.[45] In attempting to fit the absolute magnitude and shape of the data in Fig. 3 or Fig. 15, only two regions of solution for the vector couplings are found, one corresponding to constructive interference between the pion-exchange and the vector-exchange amplitudes in the forward direction and a ratio of tensor (Pauli) coupling to vector (Dirac) coupling, $G_T/G_V \simeq -0.2$–0, and the other, destructive interference and $G_T/G_V \simeq 0.5$–1.0.

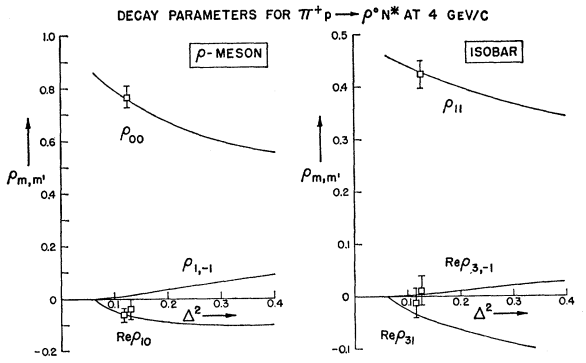

FIG. 14. The density-matrix elements $\rho_{mm'}$, appearing in (5) and (6), for decay of the ρ meson and the N^* isobar as functions of Δ^2 for the reaction $\pi^+p(\pi)\rho^0N^{*++}$. The experimental points are preliminary results of Ref. 10, averages over all Δ^2, plotted arbitrarily at the observed average value of Δ^2.

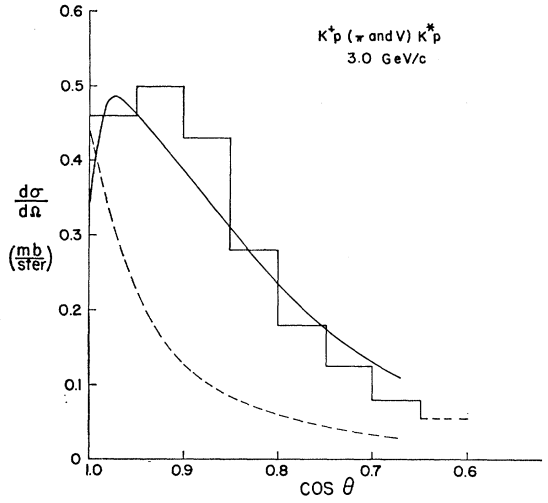

FIG. 15. Differential cross section for the reaction $K^+p(\pi$ and $V)$ $K^{*+}p$ at 3 GeV/c. The histogram represents the data of Ref. 4 (see also Fig. 3). The dashed curve is the theoretical result for pion exchange alone. The solid curve is calculated assuming a mixture a mixture of pion exchange and vector meson exchange, as discussed in the text.

The solid curve in Fig. 15 is that for one of the possible solutions for the vector-exchange couplings. In the notation of Ref. 21, the product of the squares of the dimensionless coupling constants for the $K^+V^0K^{*+}$ vertex and the pV^0p vertex is $(f^2/4\pi)\times(G_V^2/4\pi)=29$ and $G_TG_V \simeq 0.9$. The allowable variations around these values and the corresponding fits to the K^-p data are discussed in Ref. 45. The averaged decay correlation parameters are in reasonable agreement with the values quoted in Sec. 3. But more important is the fact that the momentum transfer dependence of the density matrix elements is quite marked and in accord with observation. Figure 16 gives a comparison between theory and experiment.[4] The points represent the experimental values for three different production angular intervals, while the solid curves are the theoretical predictions of the peripheral model with absorption.

The dashed curves in Fig. 16 are those expected from the peripheral model with form factors rather than absorption as the mechanism of damping the large momentum transfers. In the peripheral model with form factors the pion- and vector-meson-exchange contributions do not interfere.[21] Consequently the value of ρ_{00} is just given by $\sigma_\pi/(\sigma_\pi+\sigma_V)$, where σ_π and σ_V are the pion- and vector-meson-exchange cross sections. The dashed curves in Fig. 16 were obtained using σ_π and σ_V calculated from the peripheral model, with absorption as the source of the form factors. The curve for ρ_{00} is in definite disagreement with experiment. While it is true that the form factors for pion exchange

[52] G. Goldhaber, paper presented at the Conference on Particle and High Energy Physics, Boulder, Colorado, 1964 (unpublished).

[53] In the notation of Ref. 21 the coupling constants are $g^2/4\pi \simeq 0.75$ for the $K^+\pi^0K^{*+}$ vertex and $G^2/4\pi=14.5$ for the $p\pi^0p$ vertex. Note that there is an additional over-all factor of $\frac{2}{3}$ in the cross section because only the decay mode $K^{*+}\to K^0\pi^+$ is observed in the experiment of Ref. 4.

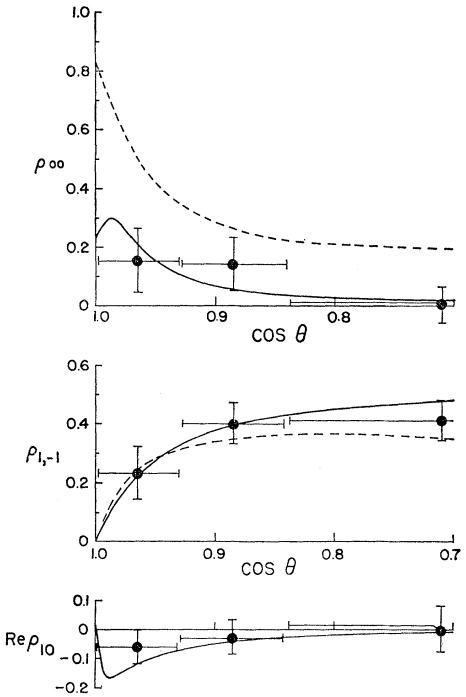

FIG. 16. Density-matrix elements $\rho_{mm'}$ for the K^* vector meson as a function of production angle for the reaction of Fig. 15. The experimental points are those of Ref. 4. The dashed curves are from the peripheral model with form factors; the solid curves are from the peripheral model including absorption.

and vector meson exchange can be adjusted relatively in such a way as to alter the shape of the decay correlation curves in Fig. 16 without destroying the agreement to the angular distribution of production in Fig. 15, there are connections between the density-matrix elements that preclude arbitrary alterations. For example, when $|G_T/G_V| \lesssim 1$ one can show that

$$\rho_{1,-1} \simeq \tfrac{1}{2}(1-\rho_{00}).$$

Thus, if the form factors are adjusted so that the calculated values of ρ_{00} agree with experiment, the theoretical results for $\rho_{1,-1}$ will tend to be too large, especially at the smallest angles of production.

KN(π and V)K*N, $Q_{ex}=0$ and $Q_{ex}=1$

In the previous example of K^* production the charge of the exchanged particle was zero. Consequently it is not directly known what mixture of $T=0$ and $T=1$ vector mesons occurs in the vector-exchange amplitude. But the empirical fact that the acceptable domain of vector couplings had a small Pauli term ($|G_T/G_V| \leq 1$) implies that the isoscalar exchanges are important. If isovector–vector-meson exchanges were dominant, one would expect G_T/G_V to be positive and large, in analogy with the large isovector anomalous magnetic moment of the nucleons. Direct experimental verification of this conclusion is obtained by the study of K^+d reactions, as already discussed in Sec. 3, where it is found that a mixture of pion and vector exchange occurs for $Q_{ex}=0$ and only pion exchange is evident for $Q_{ex}=\pm 1$.

The curves shown in Fig. 8 are calculated with the present model, assuming that for $Q_{ex}=0$ the pion- and vector-exchange coupling strengths are the same as found at 3 GeV/c (but using the absorptive parameters appropriate for 2.3 GeV/c), while for $Q_{ex}=-1$ only pion exchange occurs. The agreement between theory and experiment in each reaction is generally satisfactory for both production angular distribution and decay correlations when allowance is made for the somewhat limited statistics. There may be some evidence that a larger vector-exchange coupling would give a better fit to the $Q_{ex}=0$ data. The theoretical total cross sections (for $\Delta^2<20\mu^2$) are 0.5 mb for $K^+p\to K^{*+}p$ (into $K^0\pi^+p$) and 1.3 mb for $K^+n\to K^{*0}p$ (into $K^+\pi^-p$).

7. CONCLUDING REMARKS

The peripheral model including absorptive effects has been shown to give a remarkably good description of many quasi-two-body reactions involving the production of one or two unstable resonances in the energy range of a few GeV. The peripheral aspect of the production process has been shown to come in large part from the collimation produced by the absorption of the low partial waves. Although very important for the collimation, the absorption modifies but does not destroy an essential feature of the peripheral model, the characteristic decay correlations which result from the exchanges of definite angular momentum states in the t channel. In fact the modifications are generally in agreement with what is observed, that is, close to the predictions of the simple one-meson-exchange model at small momentum transfers and departing progressively from those values at larger production angles (e.g., see Figs. 14 and 16). A striking exception to this trend is the reaction, $\pi^+n\to\omega p$, for which the observed decay correlations are not even remotely as expected. Absorption gives at least a semiquantitative explanation.[45]

In spite of, or perhaps because of, the successes of the model several cautionary and qualifying remarks must be made. The first concerns absolute cross sections and coupling constants. When the coupling constants are known, it is found, with some notable exceptions to be discussed below, that the absolute magnitudes of the calculated cross sections, as well as the Δ^2 shapes and decay correlations, are in agreement with experiment. This gives hope that hitherto unknown coupling constants can be established by comparison of theory and experiment. But the absorptive effects are generally large enough and the uncertainties and inaccuracies

of the present model great enough that coupling constants for anything except pion exchange cannot be deduced with more than order-of-magnitude accuracy. For pion exchange the couplings are usually already known from other processes.

A conclusion that follows a fortiori from the difficulty of determining coupling constants is that vertex form factors can be disentangled from absorptive effects only with great difficulty. The model described here is based on the extreme assumption of point couplings in the simple one-meson-exchange diagram. Most of the data do not demand the presence of structure in the vertices, although some type of form factor with modest variation in Δ^2 undoubtedly exists for each vertex. There are even vertices for which rather rapidly changing form factors probably exist. The most likely candidate is the ρNN^* vertex[54] shown in Fig. 17. The triangle diagram has an anomalous threshold in the mass of the virtual ρ meson that lies very close to the physical region of a production reaction involving ρ exchange. This gives the vertex a large spatial structure or equivalently a rapidly varying form factor. It is suggestive that the production reaction $\pi^+p\to\pi^0N^{*++}$ can be considered a failure of the present model since the experimental momentum transfer distributions are very peripheral,[33] much more peripheral than those calculated using ρ-exchange with point couplings.[45] But the anomalous threshold argument runs into difficulty with the closely related reaction, $K^+p\to K^0N^{*++}$, for which the present model works well.

One remaining general question is why does a model that is basically the distorted-wave Born approximation work as well as it does for absolute cross sections. It is known that lowest order approximations may often contain features (such as decay correlations) in accord with experiment, but that absolute magnitudes are another matter. When the interaction is strong the lowest order result is often too large, sometimes to a degree that is inconsistent with unitarity. That the one-meson-exchange diagrams violate unitarity in the lowest partial waves has been known for a long time. Figure 18 shows one example of this phenomenon, the

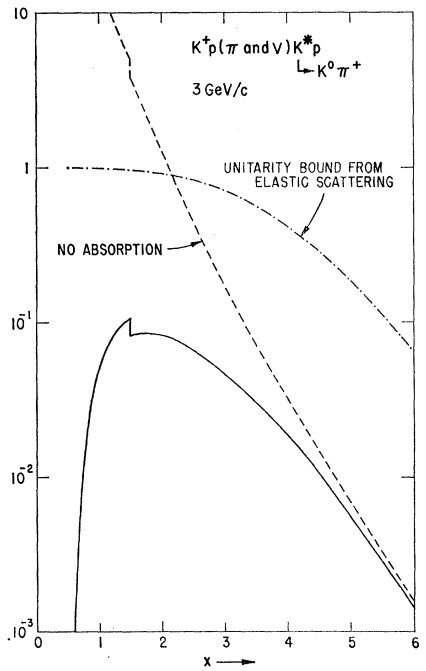

FIG. 18. Partial-wave cross section divided by the absolute unitarity bound $(2j+1)\pi/q^2$ as a function of $x=j+\frac{1}{2}$ for the reaction $K^+p(\pi$ and $V)K^{*+}p$ at 3 GeV/c. The dashed curve is the result for the simple peripheral model without absorption; the solid curve includes absorptive effects according to (19) with $\gamma_1=\gamma_2$. The absolute unitarity bound is unity on this figure; also shown is the limit inferred from the elastic scattering. The irregular behavior at small x comes from the presence of anomalous terms in the partial wave expansions (see Ref. 41).

K^* production process of Fig. 15. The dashed curve gives the partial-wave cross sections[55] for the unmodified peripheral model as a function of $x=j+\frac{1}{2}$. These are larger than the unitarity bound for the first two or three j values. But when absorptive effects are included, as shown by the solid curve, the partial-wave cross sections lie an order of magnitude or more below the unitarity limits for all j. This presumably means that if a properly unitary calculation were made the corrections would be small, and so gives a rationale for the agreements found with experiment on absolute magnitudes. A backhanded confirmation of this is probably to be found in the reaction $K^+p\to K^*N^*$ at 3 GeV/c where the theoretical cross section, assuming pion exchange, is a factor of two or more larger than experiment. The figure corresponding to Fig. 18 has the partial cross sections *with* absorption within 25% of the unitarity bound for all j values. Presumably unitarity corrections will be important here, although other effects such as intrinsic vertex factors, interference with vector-meson exchange, etc., may enter. A calculation of the many channels open to K^+p at 3 GeV/c is in

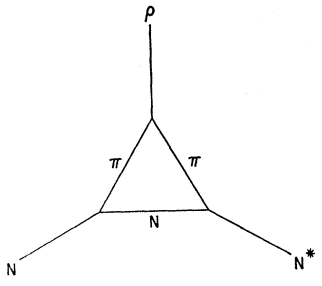

FIG. 17. Triangle diagram for the ρNN^* vertex.

[54] The author is indebted to Dr. Ian Barbour for bringing this point to his attention and stressing the importance of anomalous thresholds.

[55] The quantity plotted is actually the ratio of the partial wave cross section to the absolute upper bound, $(2j+1)\pi/q^2$, allowed by unitarity. See Eq. (3.13) of Ref. 41.

progress at CERN with a variant of the present model that incorporates unitarity explicitly.[56]

As a final remark on the limitations of the model, a well-known problem concerning vector-meson exchange (and the exchange of higher spin states) should be mentioned. At high energies an amplitude involving a t channel state of angular momentum J is proportional to s^J, where s is the square of the total energy in the center of mass. Consequently there will eventually be a violation of unitarity for vector and higher spin exchanges, whatever the coupling constants. In the energy range of interest in the present paper, there is generally not a violation of the unitarity bound, but the amplitudes do increase with increasing energy. The absorptive model of Sec. 5 modifies the amplitude in a manner that depends on the elastic scattering in the initial and final states, but to the extent that the elastic-diffraction peak does not change shape in Δ^2 with energy, the modifications affect only the Δ^2 dependence, not the s dependence. For the reaction $\pi^+p(\rho)\pi^0N^{*++}$ with a cross section that decreases with increasing energy, this difficulty has already been noted[33] in the context of the one-meson-exchange model with form factors, and it is discussed in detail for various reactions with the present model in Ref. 45. There is a hint of these difficulties in the comparison between theory and experiment shown in Fig. 8, where there is an indication that more vector exchange is needed for $Q_{ex}=0$ at 2.3 GeV/c than is given by the coupling constants determined at 3 GeV/c. The problems associated with the exchange of systems with $J>0$ are not the exclusive property of the peripheral model with absorption and should not be considered a basic limitation of the model as such. But it should be emphasized that inclusion of the absorptive effects does nothing to alleviate these difficulties. The solution presumably lies in the direction of a better description of the t-channel states (e.g., Regge poles).

ACKNOWLEDGMENTS

Much of this paper is based on work done in collaboration with K. Gottfried and others at CERN during the academic year 1963–64 while the author was a Ford Foundation Fellow on sabbatical leave from the University of Illinois. The author wishes to take this opportunity to thank Professor Gottfried for a most fruitful collaboration, still in progress, and to express his gratitude to CERN for the award of the fellowship and to Professor V. F. Weisskopf and Professor L. Van Hove for their kind hospitality during his stay.

[56] K. Dietz and H. Pilkuhn (private communication).

Discussion

GUTH: (*Editor's comment:* The exact wording of Dr. Guth's question concerning the Born approximation was lost in process of transcription.)

JACKSON: I should probably go back to Dalitz' remark that it is not quite the Born approximation. The amplitude is a particular Feynman graph which, at small momentum transfers, can be argued to be the main contribution. When one looks in the t channel at which mass states can contribute, where pi exchange occurs quite often the next possibility is omega exchange. At momentum transfers which are well below the square of the omega mass, you may expect that the pion-exchange diagram is the dominant feature. Concerning unitarity, I merely wanted to observe that when the absorptive effects are included, the amplitudes do not violate unitarity, as they do in the low partial waves without absorptive effects.

In some of the reactions we have difficulty fitting the delta-squared distribution, and it is in just those reactions that we are very close to the unitarity bound. For such reactions one may have to do a more elaborate K-matrix calculation, where the unitary property is incorporated in a way that is not just accidental, as occurs with absorption.

ZUPANČIČ: Have Ferrari and Amaldi any physical idea of what the delta dependence is due to?

JACKSON: There are expected to be renormalization effects which will give factors that depend on delta squared. There are, in fact, three factors, one from each vertex, and one from the propagator, which are functions of delta squared. The argument of Ferrari and Selleri was that we don't know how to calculate those things, so we will lump them all into one, and just use an empirical expression. The criticism is that, when one makes plausible estimates of the kind of variation that would occur from such vertex corrections, it is much less violent than seems to be necessary to fit the experimental delta-squared distributions.

GRIFFY: Wouldn't it be possible to have an interference, say between a pi and an omega, which would lead to a lower effective mass, just as one does with the isospin nucleon form factor? Could you add together the pi and omega?

JACKSON: In the rho-production reaction there is no interference between poin exchange and vector meson exchange in the unmodified peripheral model. Pion exchange populates the spin state $m=0$, while vector-meson exchange populates $m=\pm1$. Adding in vector-meson exchange will only raise the cross section at wide angles even more. In reactions with only vector meson exchange there is the possibility of interference between contributions from the different vector mesons, but with the known masses it is difficult to produce much of an effect.